Deciphering Cosmic-Ray Anisotropies

Markus Ahlers

Niels Bohr Institute, Copenhagen

CEA-Saclay Seminar Series

February 14, 2022

The Niels Bohr International Academy

VILLUM FONDEN

UNIVERSITY OF COPENHAGEN

Galactic Cosmic Rays

- *Standard paradigm:* Galactic CRs accelerated in **supernova remnants**

✔ sufficient power: $\sim 10^{-3} \times \mathrm{M}_\odot$ with a rate of ~ 3 SNe per century
[Baade & Zwicky'34]

- galactic CRs via diffusive shock acceleration?

$$n_{\rm CR} \propto E^{-\gamma} \qquad \text{(at source)}$$

- energy-dependent **diffusion** through Galaxy

$$n_{\rm CR} \propto E^{-\gamma-\delta} \qquad \text{(observed)}$$

- arrival direction **mostly isotropic**

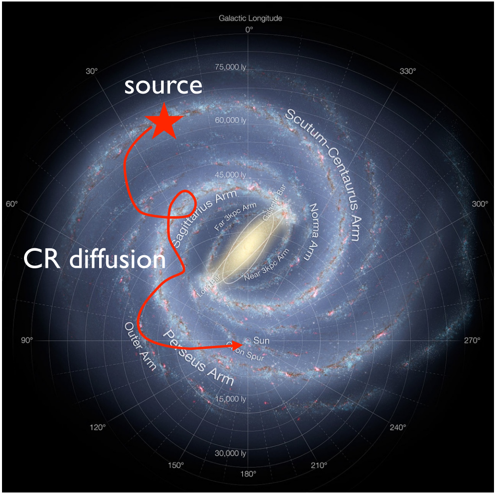

Galactic Cosmic Ray Anisotropy

Cosmic ray anisotropies up to the level of **one-per-mille** at various energies
(Super-Kamiokande; Milagro; ARGO-YBJ; EAS-TOP, Tibet AS-γ; IceCube; HAWC)

Anisotropy = Relative Intensity - 1

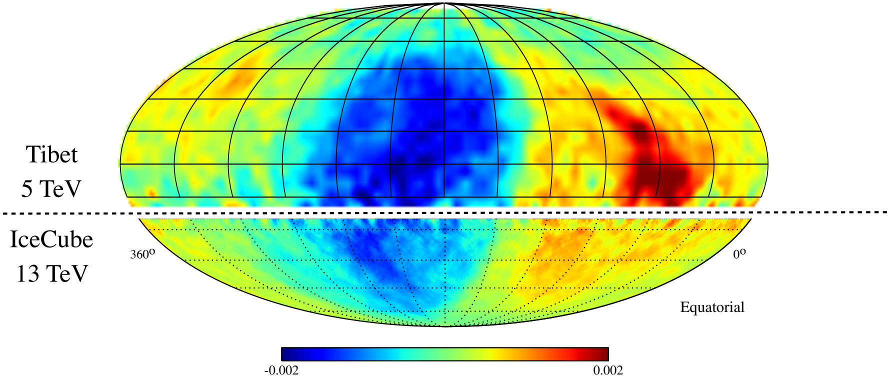

[*e.g.* review by MA & Mertsch'16]

Galactic Cosmic Ray Anisotropy

Cosmic ray anisotropies up to the level of **one-per-mille** at various energies
(Super-Kamiokande; Milagro; ARGO-YBJ; EAS-TOP, Tibet AS-γ; IceCube; HAWC)

Energy-Dependence

Large-scale (dipole) anisotropy has strong energy dependence
with phase-flip around 100 TeV.

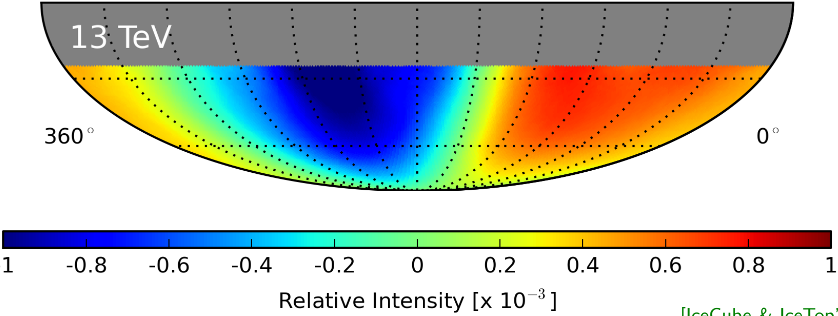

[IceCube & IceTop'16]

Energy-Dependence

Large-scale (dipole) anisotropy has strong energy dependence with phase-flip around 100 TeV.

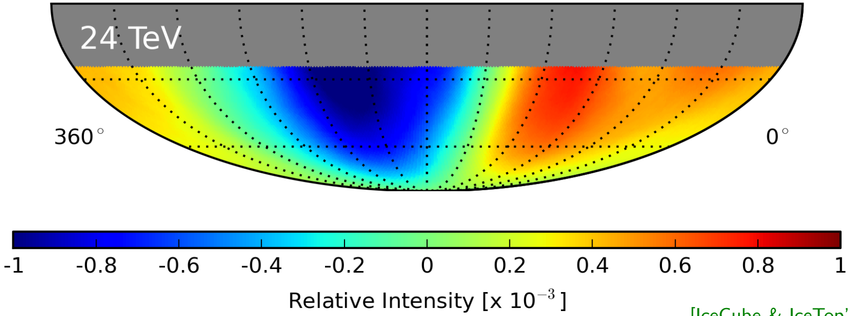

[IceCube & IceTop'16]

Energy-Dependence

Large-scale (dipole) anisotropy has strong energy dependence
with phase-flip around 100 TeV.

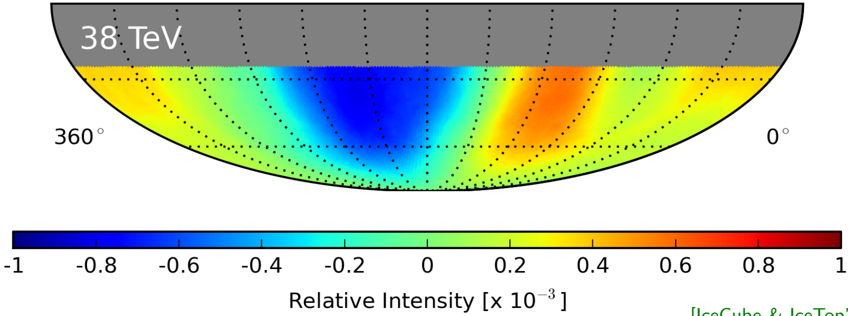

[IceCube & IceTop'16]

Energy-Dependence

Large-scale (dipole) anisotropy has strong energy dependence
with phase-flip around 100 TeV.

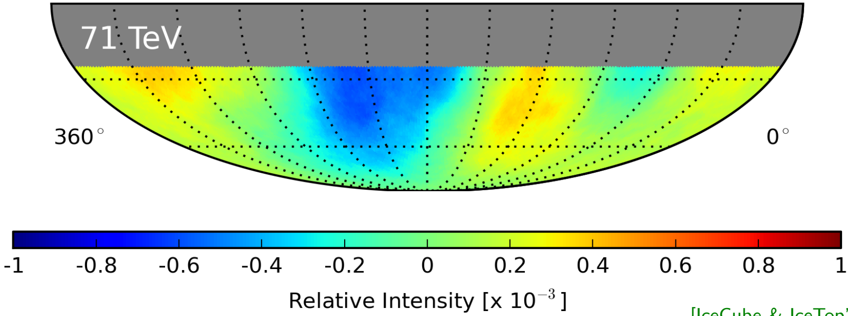

[IceCube & IceTop'16]

Energy-Dependence

Large-scale (dipole) anisotropy has strong energy dependence
with phase-flip around 100 TeV.

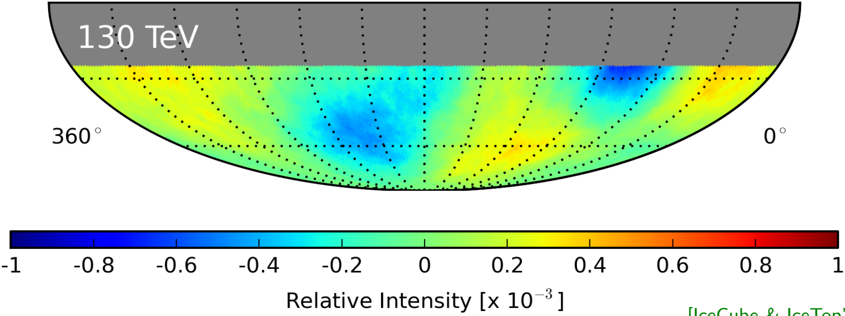

[IceCube & IceTop'16]

Energy-Dependence

Large-scale (dipole) anisotropy has strong energy dependence
with phase-flip around 100 TeV.

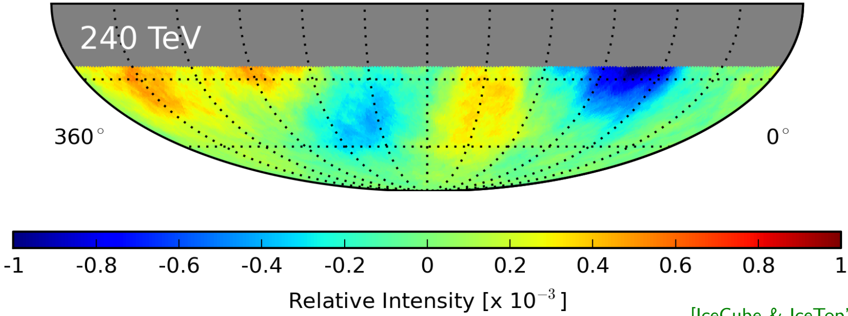

[IceCube & IceTop'16]

Energy-Dependence

Large-scale (dipole) anisotropy has strong energy dependence
with phase-flip around 100 TeV.

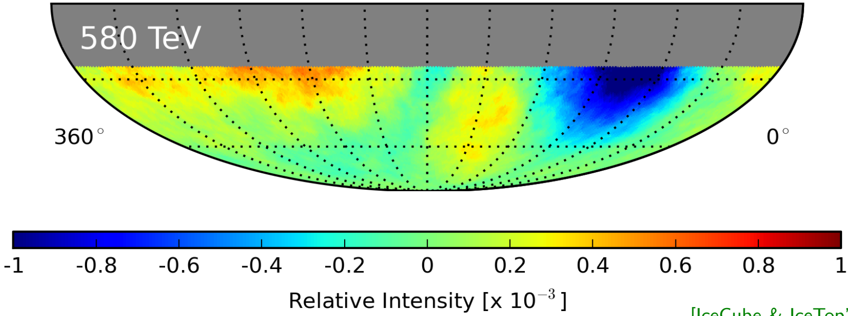

[IceCube & IceTop'16]

Energy-Dependence

Large-scale (dipole) anisotropy has strong energy dependence
with phase-flip around 100 TeV.

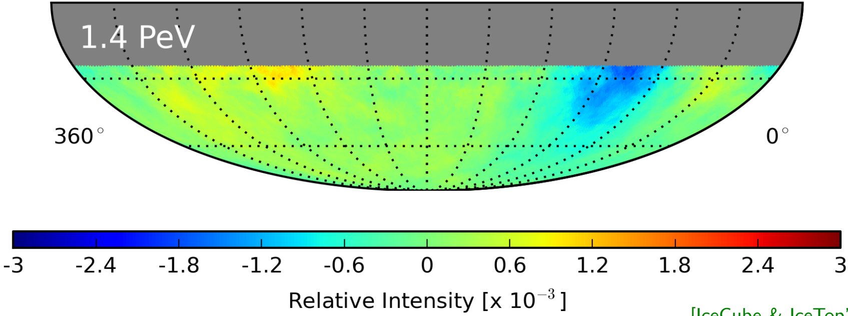

[IceCube & IceTop'16]

Energy-Dependence

Large-scale (dipole) anisotropy has strong energy dependence
with phase-flip around 100 TeV.

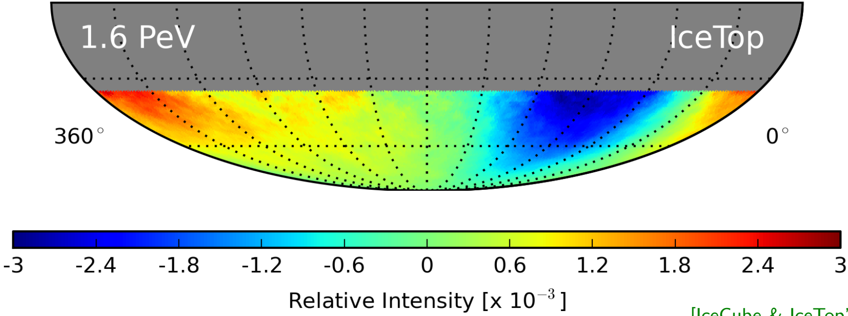

[IceCube & IceTop'16]

Energy-Dependence

Large-scale (dipole) anisotropy has strong energy dependence
with phase-flip around 100 TeV.

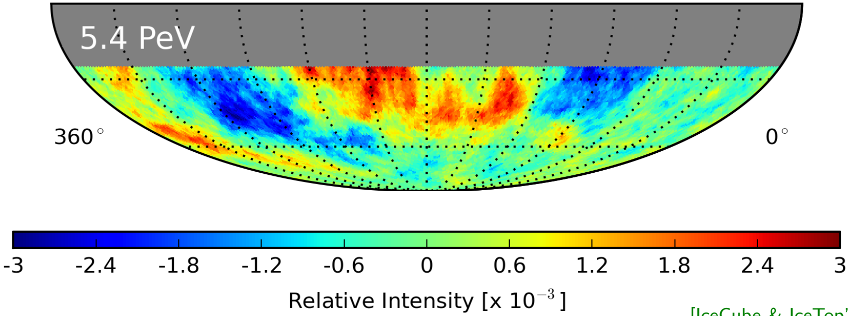

[IceCube & IceTop'16]

Time-Dependence

No significant variation of TeV-PeV anisotropy over time scales of $\mathcal{O}(10)$ years.

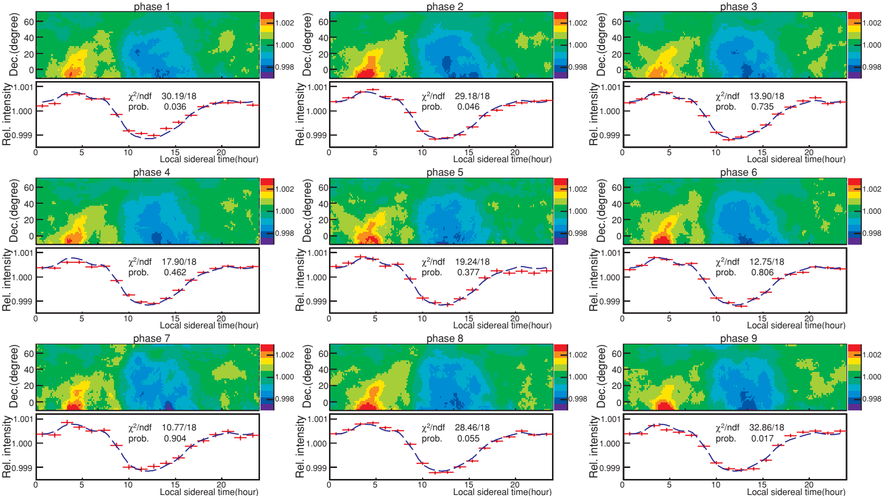

[Tibet-ASγ'10]

Dipole Anisotropy at 8 EeV

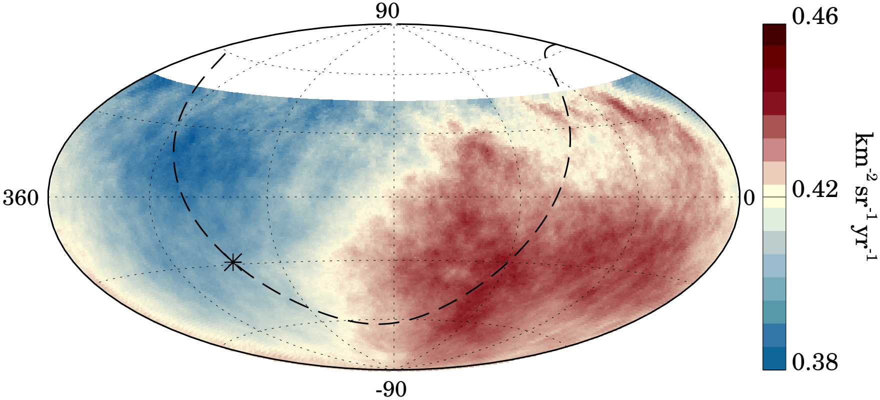

Energy [EeV]	Dipole component d_z	Dipole component $d_\perp$	Dipole amplitude d	Dipole declination δ_d [°]	Dipole right ascension α_d [°]
4 to 8	-0.024 ± 0.009	$0.006^{+0.007}_{-0.003}$	$0.025^{+0.010}_{-0.007}$	-75^{+17}_{-8}	80 ± 60
8	-0.026 ± 0.015	$0.060^{+0.011}_{-0.010}$	$0.065^{+0.013}_{-0.009}$	-24^{+12}_{-13}	100 ± 10

[Auger, Science'17]

Anisotropy Reconstruction

Reconstruction Methods

✘ data is strongly **time-dependent**:

- detector deployment/maintenance
- atmospheric conditions (day/night, seasons)
- power outages,. . .

✘ **local anisotropies** of detector:

- detector geometry
- mountains
- geo-magnetic fields,. . .

- two analysis strategies:
  - **Monte-Carlo & monitoring** (limited by **systematic** uncertainties)
  - **data-driven likelihood methods** (limited by **statistical** uncertainties)

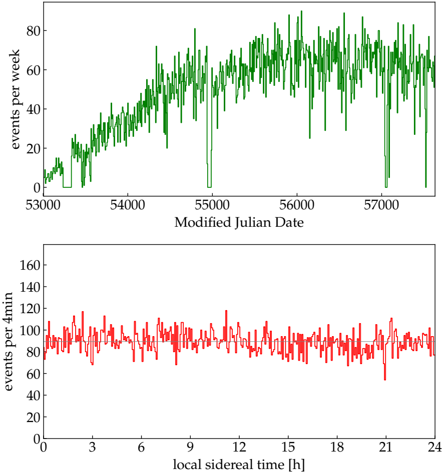

example: Auger data > 8 EeV

[MA'18]

East-West Method

- Strong time variation of cosmic ray background level can be compensated by differential methods. [*e.g.* Bonino *et al.*'11]
- **East-West asymmetry:**

$$A_{\rm EW}(t) \equiv \frac{N_{\rm E}(t) - N_{\rm W}(t)}{N_{\rm E}(t) + N_{\rm W}(t)} \simeq \underbrace{\Delta\alpha \frac{\partial}{\partial\alpha}\delta I(\alpha,0)}_{\textbf{if dipole!}} + \underbrace{\text{const}}_{\text{local asym.}}$$

- For instance, Auger data > 8 EeV:

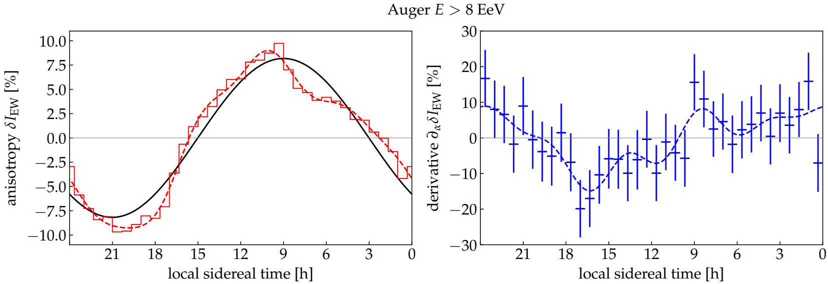

- best-fit dipole from EW method: $d_\perp = (8.2 \pm 1.4)\%$ and $\alpha_d = 135^\circ \pm 10^\circ$

Issues with Data-Driven Reconstruction

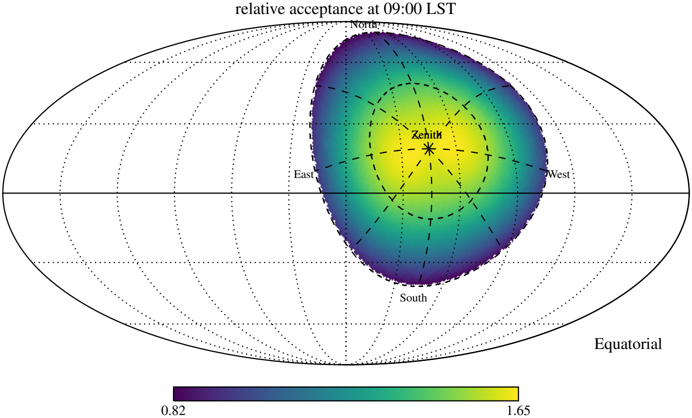

- ground-based detectors need to be **calibrated** by CR data
- true CR dipole defined by amplitude A_1, and orientation (RA,DEC) $= (\alpha_1,\delta_1)$

✘ observable: **projected dipole** with amplitude $A'_1 = A_1 \cos\delta_1$ and orientation $(\alpha_1,0)$

[Iuppa & Di Sciascio'13; MA *et al.*'15]

Issues with Data-Driven Reconstruction

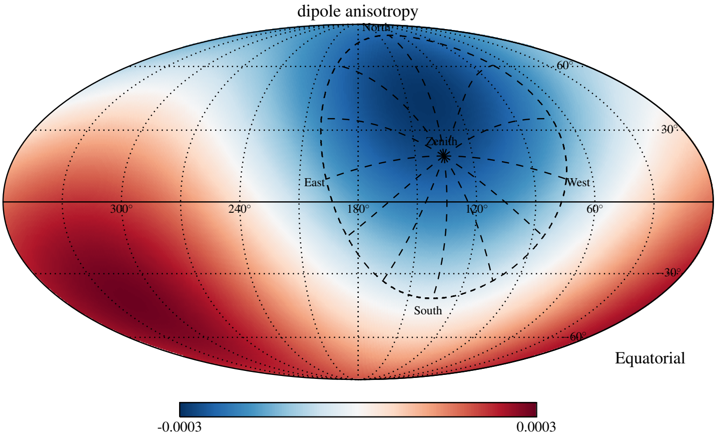

- ground-based detectors need to be **calibrated** by CR data
- true CR dipole defined by amplitude A_1, and orientation (RA,DEC) $= (\alpha_1,\delta_1)$

✗ observable: **projected dipole** with amplitude $A_1' = A_1 \cos\delta_1$ and orientation $(\alpha_1,0)$

[Iuppa & Di Sciascio'13; MA *et al.*'15]

Issues with Data-Driven Reconstruction

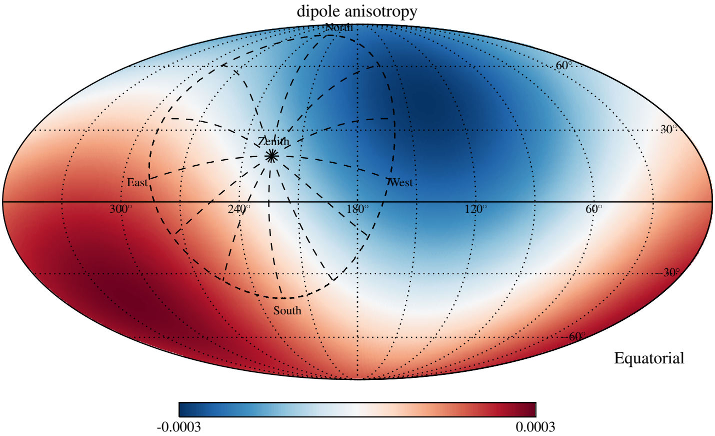

- ground-based detectors need to be **calibrated** by CR data
- true CR dipole defined by amplitude A_1, and orientation (RA,DEC) $= (\alpha_1,\delta_1)$

✘ observable: **projected dipole** with amplitude $A'_1 = A_1 \cos\delta_1$ and orientation $(\alpha_1,0)$

[Iuppa & Di Sciascio'13; MA *et al.*'15]

Issues with Data-Driven Reconstruction

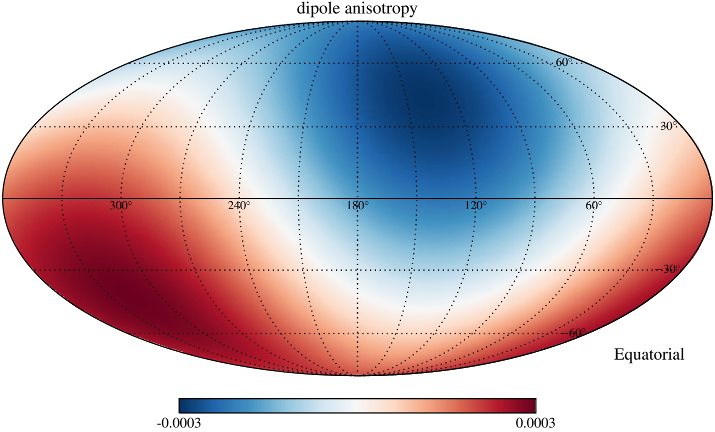

- ground-based detectors need to be **calibrated** by CR data
- true CR dipole defined by amplitude A_1, and orientation (RA,DEC) $= (\alpha_1,\delta_1)$

✘ observable: **projected dipole** with amplitude $A_1' = A_1 \cos\delta_1$ and orientation $(\alpha_1,0)$

[Iuppa & Di Sciascio'13; MA *et al.*'15]

Issues with Data-Driven Reconstruction

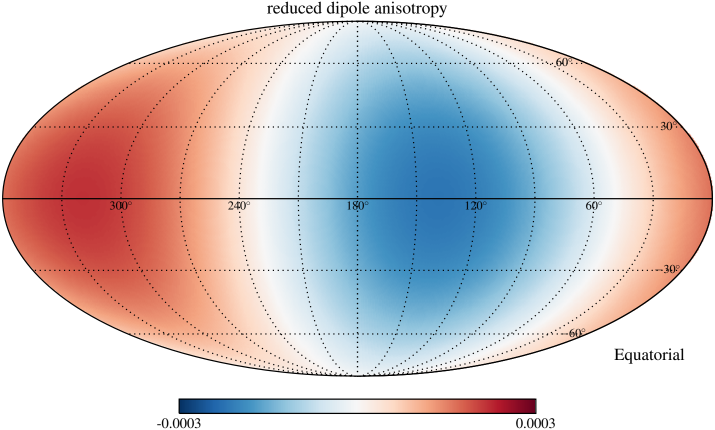

- ground-based detectors need to be **calibrated** by CR data
- true CR dipole defined by amplitude A_1, and orientation (RA,DEC) $= (\alpha_1,\delta_1)$

✘ observable: **projected dipole** with amplitude $A_1' = A_1 \cos\delta_1$ and orientation $(\alpha_1,0)$

[Iuppa & Di Sciascio'13; MA *et al.*'15]

Take-Away on Dipole Reconstruction

Data-driven methods of anisotropy reconstructions used by ground-based observatories are **only sensitive to equatorial dipole** (or, more generally, to all $m \neq 0$ multipoles)

$$\Delta\delta_\perp \sim \frac{1}{\sqrt{N_{\rm tot}}} \qquad \mathcal{N} \sim \frac{4\pi}{N_{\rm tot}}$$

Large-Scale Anisotropy

Cosmic Ray Dipole Anisotropy

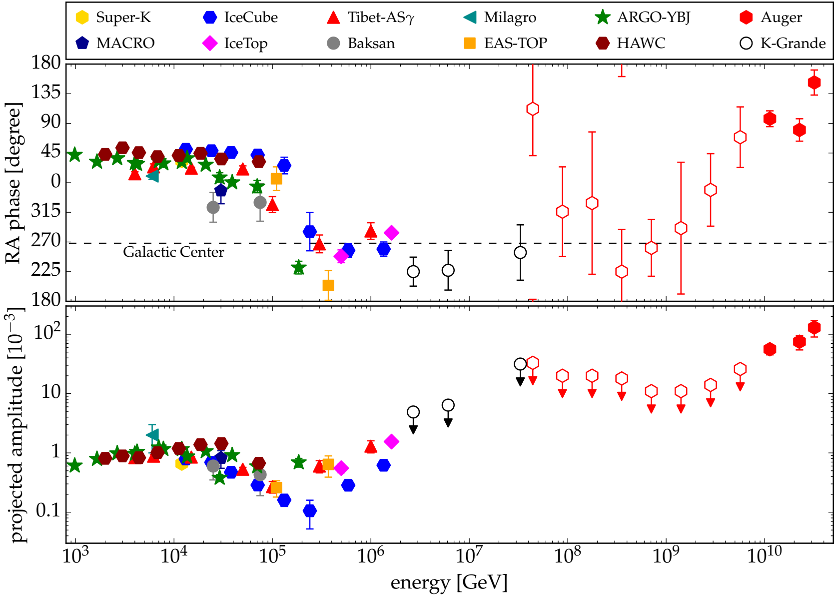

Cosmic Ray Dipole Anisotropy

- Spherical harmonics expansion of relative intensity yields:

$$I(\Omega) = 1 + \underbrace{\boldsymbol{\delta} \cdot \widehat{\mathbf{n}}(\Omega)}_{\text{dipole}} + \sum_{\ell \geq 2} \sum_m a_{\ell m} Y^{\ell m}(\Omega)$$

- cosmic ray density $n_{\rm CR} \propto E^{-\Gamma_{\rm CR}}$ and dipole vector $\boldsymbol{\delta}$ from **diffusion theory**:

$$\underbrace{\partial_t n_{\rm CR} \simeq \nabla(\mathbf{K}\nabla n_{\rm CR}) + Q_{\rm CR}}_{\text{diffusion equation}} \quad \text{and} \quad \underbrace{\boldsymbol{\delta} \simeq 3\mathbf{K}\nabla n_{\rm CR}/n_{\rm CR}}_{\text{from Fick's law}}$$

- diffusion tensor $\mathbf{K}$ in general anisotropic (background field $\mathbf{B}$):

$$K_{ij} = \kappa_\parallel \widehat{B}_i \widehat{B}_j + \kappa_\perp (\delta_{ij} - \widehat{B}_i \widehat{B}_j) + \kappa_A \epsilon_{ijk} \widehat{B}_k$$

- **relative motion** $\mathbf{v}$ of the observer in plasma rest frame ($\star$): [Compton & Getting'35]

$$\boldsymbol{\delta} = \boldsymbol{\delta}^\star + \underbrace{(2 + \Gamma_{\rm CR})\mathbf{v}/c}_{\text{Compton-Getting effect}}$$

TeV-PeV Dipole Anisotropy

- reconstructed diffuse dipole:

$$\delta^\star = \delta - \underbrace{(2+\Gamma_{CR})\beta}_{\text{Compton-Getting}} = 3\mathbf{K}\cdot\nabla n^\star/n^\star$$

- projection onto equatorial plane: ➜

$$\delta^\star_{EP} = (\delta^\star_{0h}, \delta^\star_{6h})$$

- **strong regular magnetic fields** in the local environment

➜ diffusion tensor reduces to **projector**:
[*e.g.* Mertsch & Funk'14; Schwadron *et al.*'14]

$$K_{ij} \to \kappa_\parallel \widehat{B}_i \widehat{B}_j$$

- TeV–PeV dipole data consistent with magnetic field direction inferred by IBEX data [McComas *et al.*'09]

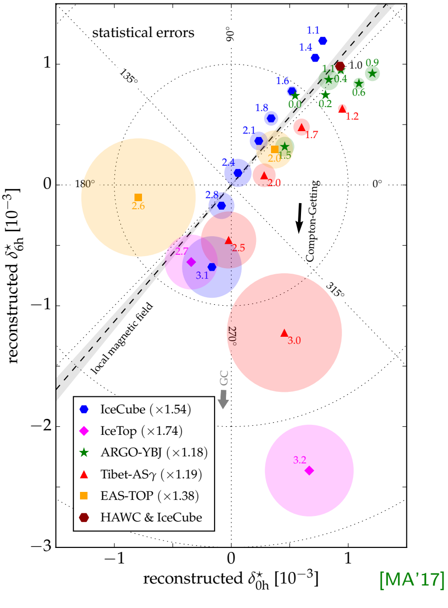

[MA'17]

Known Local Supernova Remnants

- projection maps source gradient onto $\widehat{\mathbf{B}}$ **or** $-\widehat{\mathbf{B}}$

➜ **dipole phase** α_1 depends on orientation of magnetic hemispheres

- intersection of magnetic equator with Galactic plane defines two source groups:

$$120^\circ \lesssim l \lesssim 300^\circ \to \alpha_1 \simeq 49^\circ$$

$$-60^\circ \lesssim l \lesssim 120^\circ \to \alpha_1 \simeq 229^\circ$$

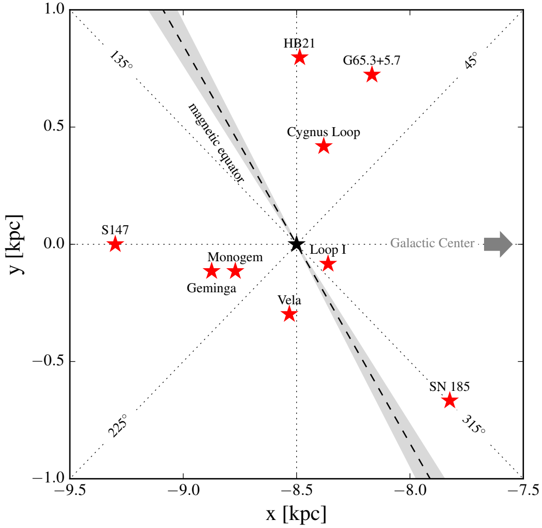

Phase-Flip by Vela SNR?

- 1–100 TeV phase indicates dominance of a local source within longitudes:

$$120^\circ \lesssim l \lesssim 300^\circ$$

- **plausible scenario: Vela SNR** [MA'16]
  - *age* : $\simeq 11,000$ yrs
  - *distance* : $\simeq 1,000$ lyrs
  - *SNR rate* : $\mathcal{R}_{\rm SNR} = 1/30\,{\rm yr}^{-1}$
  - *(effective) isotropic diffusion*:

$$K_{\rm iso} \simeq 4\times 10^{28}(E/3{\rm GeV})^{1/3}{\rm cm}^2/{\rm s}$$

  - *Galactic half height* : $H \simeq 3$ kpc
  - *instantaneous CR emission* ($Q_\star$)

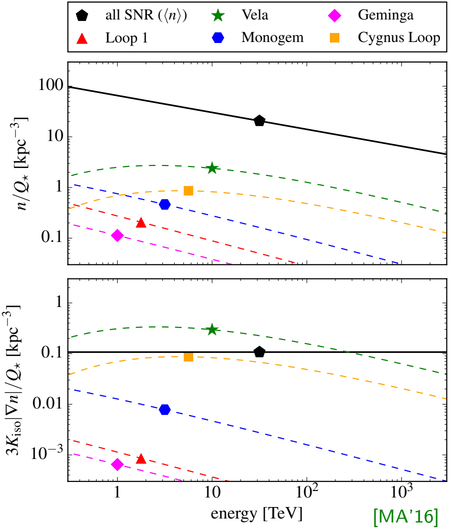

[MA'16]

Position of SNR

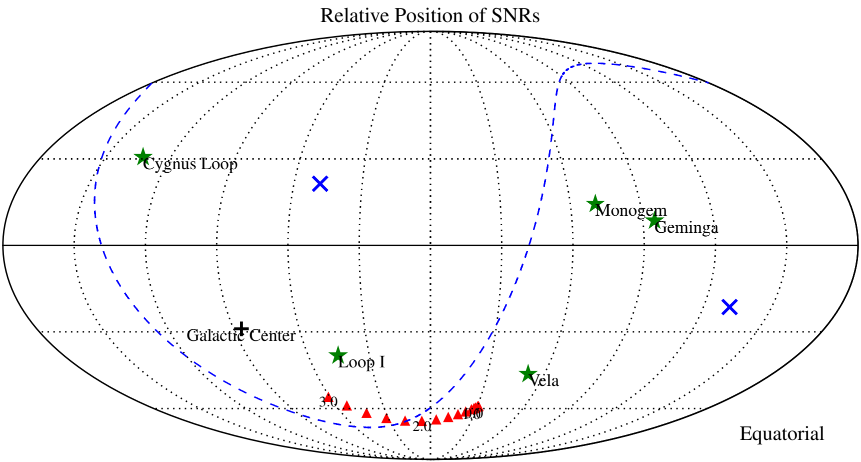

Relative position of the five closest known SNRs. The magnetic field direction (IBEX) is indicated by blue × and the **magnetic horizon** by a dashed line.

Phase-Flip by Vela SNR

- 1–100 TeV phase indicates dominance of a local source within longitudes:

$$120^\circ \lesssim l \lesssim 300^\circ$$

- **plausible scenario: Vela SNR** [MA'16]
  - *age* : $\simeq 11,000$ yrs
  - *distance* : $\simeq 1,000$ lyrs
  - *SNR rate* : $\mathcal{R}_{\rm SNR} = 1/30\,{\rm yr}^{-1}$
  - *(effective) isotropic diffusion*:

$$K_{\rm iso} \simeq 4 \times 10^{28} (E/3{\rm GeV})^{1/3} {\rm cm}^2/{\rm s}$$

  - *Galactic half height* : $H \simeq 3$ kpc
  - *instantaneous CR emission* ($Q_\star$)

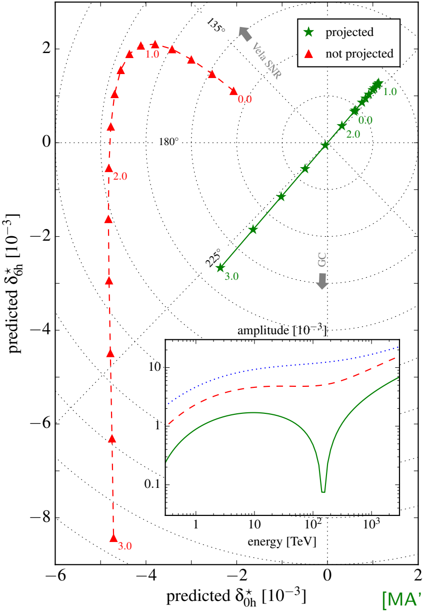

[MA'16]

Small-Scale Anisotropy

Likelihood Reconstructions

✘ Traditional "East-West method" has deficits w.r.t reconstruction of medium- and small-scale anisotropies.

➜ Alternatively, data can be analyzed to *simultaneously* reconstruct:

- **relative acceptance** $\mathcal{A}(\varphi,\theta)$ (in local coordinates)
- **relative intensity** $I(\alpha,\delta)$ (in equatorial coordinates)
- **background rate** $\mathcal{N}(t)$ (in sidereal time)

- expected number of CRs observed in sidereal time bin τ and local coordinate i:

$$\mu_{\tau i} = \mu(\mathcal{I}_{\tau i}, \mathcal{N}_\tau, \mathcal{A}_i)$$

- reconstruction via maximum likelihood:

$$\mathcal{L}(n|I,\mathcal{N},\mathcal{A}) = \prod_{\tau i} \frac{(\mu_{\tau i})^{n_{\tau i}} e^{-\mu_{\tau i}}}{n_{\tau i}!}$$

- Maximum can be reconstructed by iterative methods. [MA *et al.*'15]

➜ used in joint IceCube & HAWC analysis [IceCube & HAWC'18]

Likelihood Reconstructions

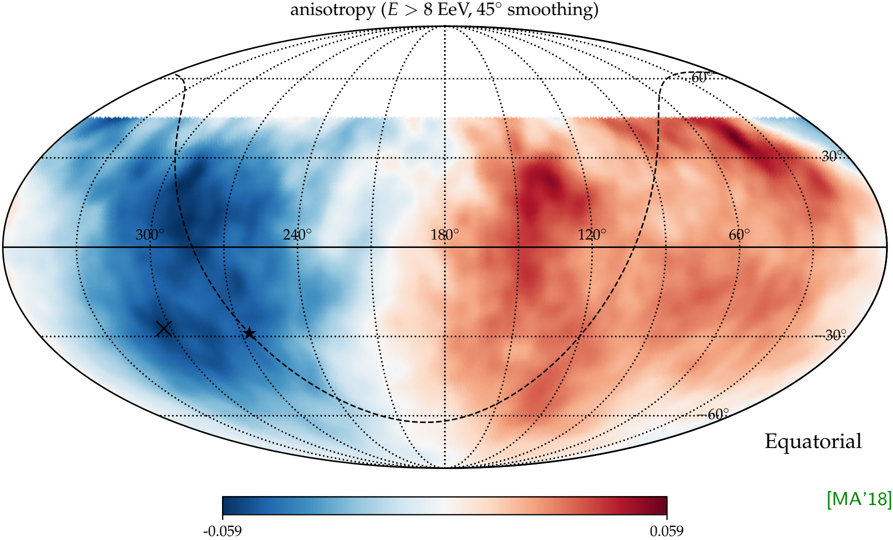

[MA'18]

Method can also be applied to high-energy data beyond the knee, *e.g.* Auger.

Likelihood Reconstructions

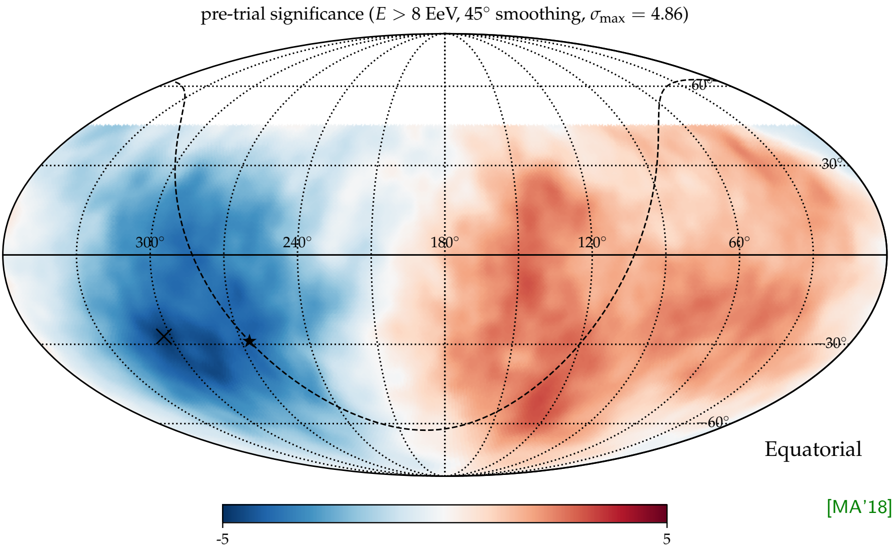

[MA'18]

Method can also be applied to high-energy data beyond the knee, *e.g.* Auger.

Small-Scale Anisotropy

- Significant TeV small-scale anisotropies down to angular scales of $\mathcal{O}(10)$ degrees.

- Strong local excess ("region A") observed by Northern observatories.

  [Tibet-ASγ'06; Milagro'08]
  [ARGO-YBJ'13; HAWC'14]

- Angular power spectra of IceCube and HAWC data show excess compared to isotropic arrival directions. [IceCube'11; HAWC'14]

$$C_\ell = \frac{1}{2\ell+1}\sum_{m=-\ell}^{\ell}|a_{\ell m}|^2$$

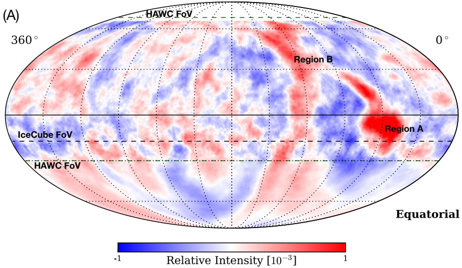

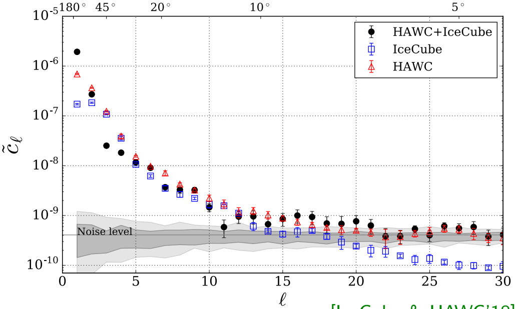

[IceCube & HAWC'18]

Small-Scale Anisotropies from Heliosphere?

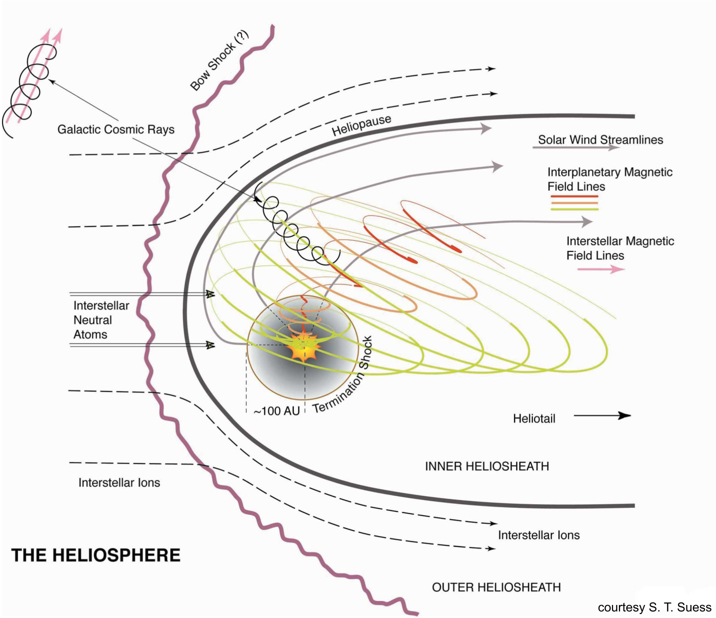

courtesy S. T. Suess

Small-Scale Anisotropies from Heliosphere?

- **Solar potential** affects cosmic ray flux (monopole) only at rigidity $\mathcal{R} \lesssim 10\,\mathrm{GV}$.

  [Gleeson & Axford'68;Gleeson & Urch'73]

- However, gyroradius of sub-TV cosmic rays smaller than the size of heliosphere:

$$r_g \simeq 200 \left(\frac{\mathcal{R}}{\mathrm{TV}}\right)\left(\frac{B}{\mu\mathrm{G}}\right)^{-1} \mathrm{AU}$$

- Various effects of cosmic transport and acceleration have been considered:
  - ⋆ hard CR spectra via magnetic reconnection in the heliotail [Lazarian & Desiati'10]
  - ⋆ non-isotropic particle transport in the heliosheath [Desiati & Lazarian'11]
  - ⋆ heliospheric electric fields induced by plasma motion [Drury'13]
  - ⋆ simulation via CR back-tracking in MHD simulation of heliosphere

    [Zhang, Zuo & Pogorelov'14; López-Barquero *et al.*'16]

Small-Scale Anisotropy from Local Turbulence

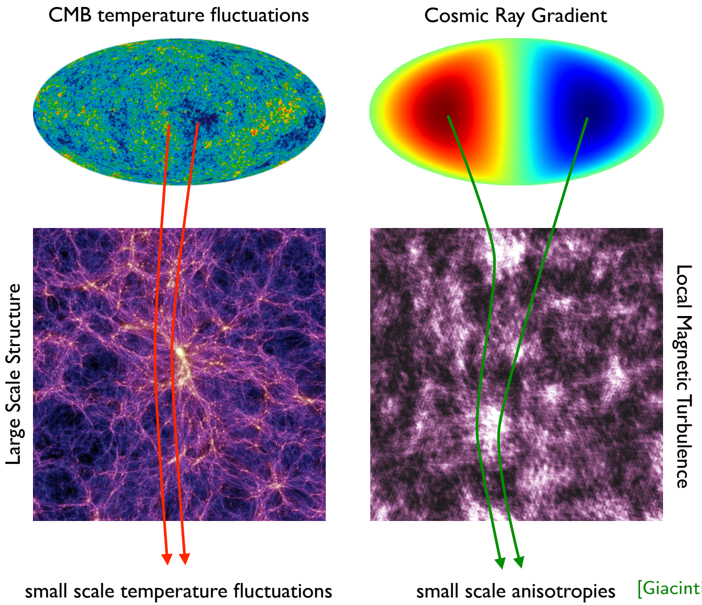

[Giacinti & Sigl'12]

Small-Scale Theorem

- *Assumptions:*
  - **absences of cosmic ray sources and sinks**
  - **isotropic and static** magnetic turbulence
  - initially, **homogeneous** phase space distribution

- *Theorem:* The sum over the ensemble-averaged angular power spectrum is constant:

$$\sum_\ell (2\ell+1)\langle C_\ell(t)\rangle = \text{const}$$

- Proof via **Liouville's theorem and angular auto-correlation function.** [MA'14]

➜ Wash-out of individual moments by diffusion (rate $\nu_\ell \propto \ell(\ell+1)$) has to be compensated by **generation of small-scale anisotropy**.

➜ Theorem implies small-scale angular features from large-scale average dipole anisotropy. [Giacinti & Sigl'12; MA'14; MA & Mertsch'15]

Comparison to CR Data

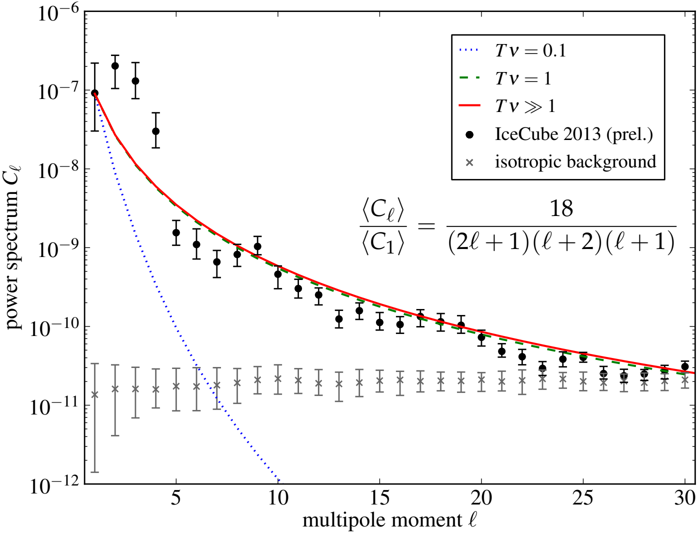

[MA'14]

Simulation via Backtracking

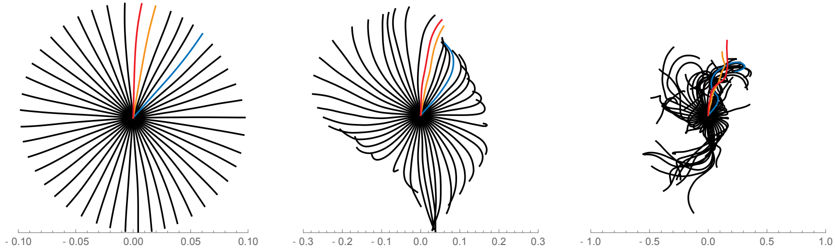

- Consider a local (quasi-)stationary solution of the **diffusion approximation**:

$$4\pi\langle f\rangle \simeq n_{\rm CR} + \underbrace{(\mathbf{r} - 3\,\widehat{\mathbf{p}}\,\mathbf{K})\nabla n_{\rm CR}}_{\text{1st order correction}}$$

- Ensemble-averaged C_ℓ's ($\ell \geq 1$): [MA & Mertsch'15]

$$\frac{\langle C_\ell\rangle}{4\pi} \simeq \int \frac{{\rm d}\hat{\mathbf{p}}_1}{4\pi}\int \frac{{\rm d}\hat{\mathbf{p}}_2}{4\pi} P_\ell(\hat{\mathbf{p}}_1\hat{\mathbf{p}}_2) \lim_{T\to\infty} \underbrace{\langle \mathbf{r}_{1i}(-T)\mathbf{r}_{2j}(-T)\rangle}_{\textit{relative}\text{ diffusion}} \frac{\partial_i n_{\rm CR}\partial_j n_{\rm CR}}{n^2_{\rm CR}}$$

Simulation via Backtracking

- simulation in isotropic & static magnetic turbulence with

$$\overline{\delta \mathbf{B}^2} = \mathbf{B}_0^2$$

- relative orientation of CR gradient:
  - solid lines : $\mathbf{B}_0 \parallel \nabla n$
  - dotted lines : $\mathbf{B}_0 \perp \nabla n$
- diffusive regime at $T\Omega \gtrsim 100$
- *enhanced* dipole predicions:

$$\langle C_1 \rangle > C_1 \text{ for } \langle f \rangle$$

- asymptotically **limited by simulation noise**:

$$\mathcal{N} \simeq \frac{4\pi}{N_{\rm pix}} 2TK^s_{ij}\frac{\partial_i n \partial_j n}{n^2}$$

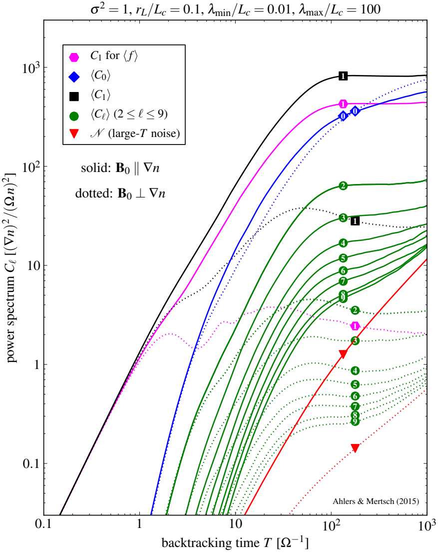

[MA & Mertsch'15]

Simulation vs. Data

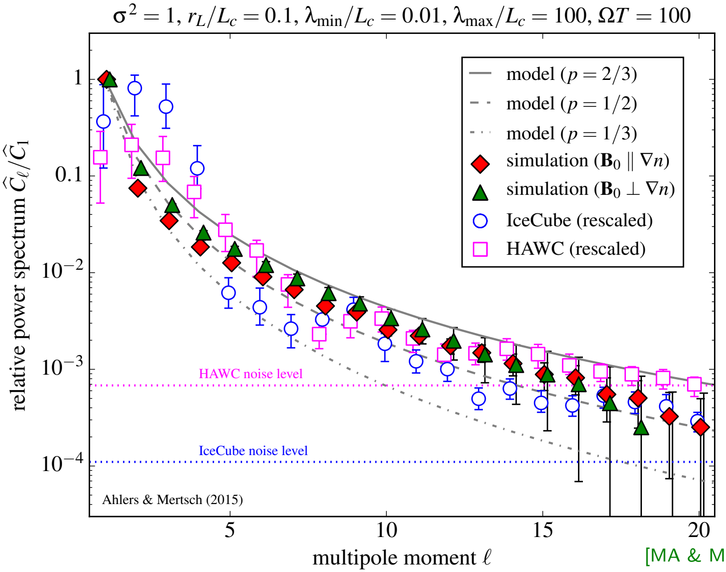

[MA & Mertsch'15]

“Via Lactea Incognita”

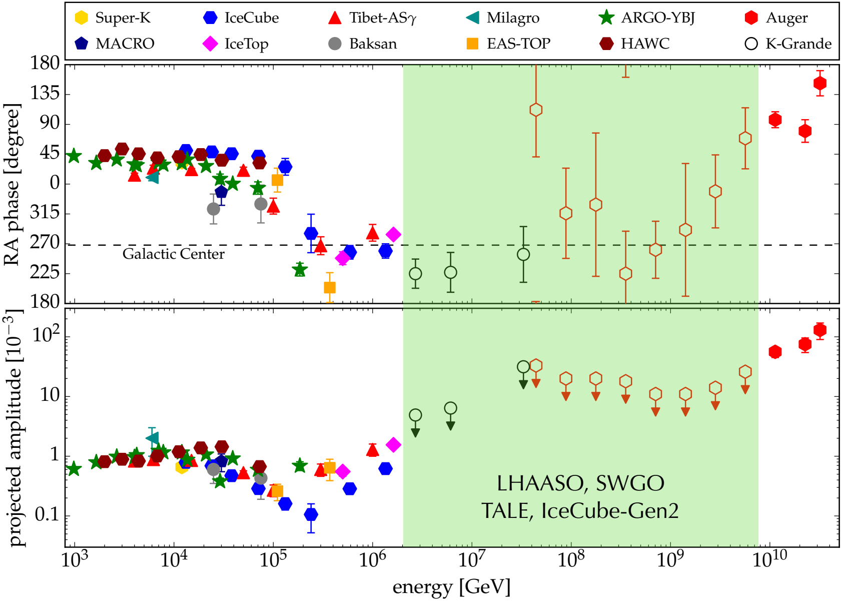

Small-Scale Features Above the Knee

- KASCADE-Grande in Karlsruhe, Germany (49.1° N, 8.4° E)
- data collected between March 2004 and October 2012
- available via: `kcdc.ikp.kit.edu`
- three energy bins from N_{ch} cuts:

data	E_{med}♣	N_{ch}-range	N_{tot}
sidereal solar	–	$\geq 10^{5.2}$	23,674,844
bin 1	2.7 PeV	$[10^{5.2}, 10^{5.6})$	17,443,774
bin 2	6.1 PeV	$[10^{5.6}, 10^{6.4})$	6,084,275
bin 3	33 PeV	$\geq 10^{6.4}$	146,795

- Full anisotropy construction in Northern Hemisphere possible with max-$\mathcal{L}$ method. [MA'19]

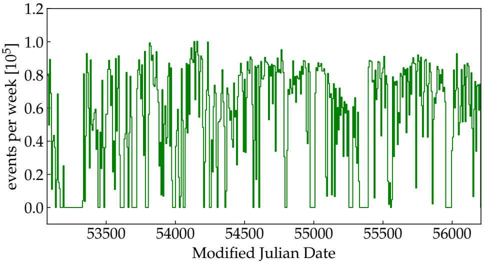

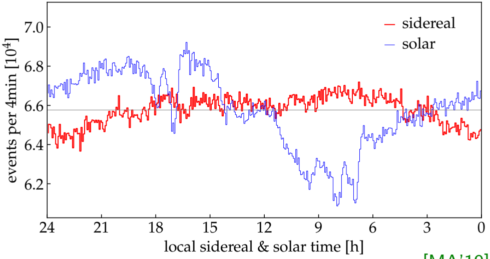

[MA'19]

Small-Scale Features Above the Knee

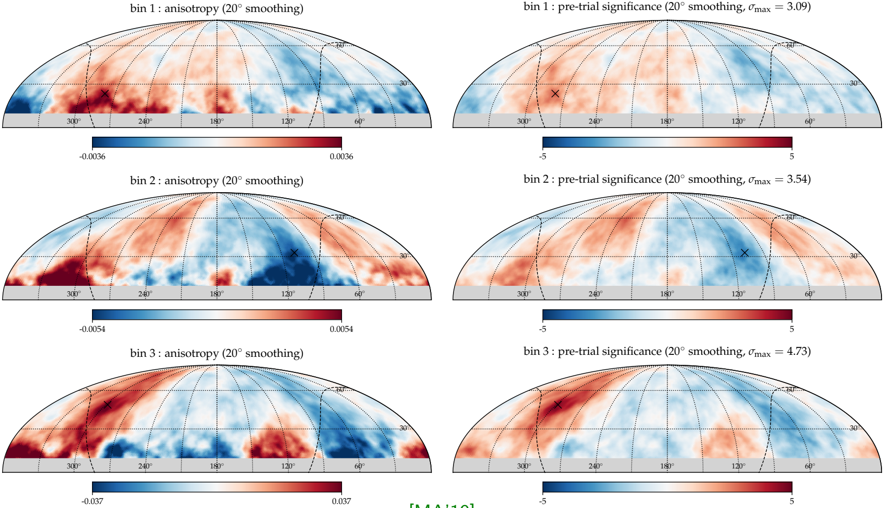

[MA'19]

Sidereal anisotropy in the KASCADE-Grande data with median energy of 2.7 PeV (bin 1), 6.1 PeV (bin 2) and 33 PeV (bin 3).

Small-Scale Feature At the 2nd Knee?

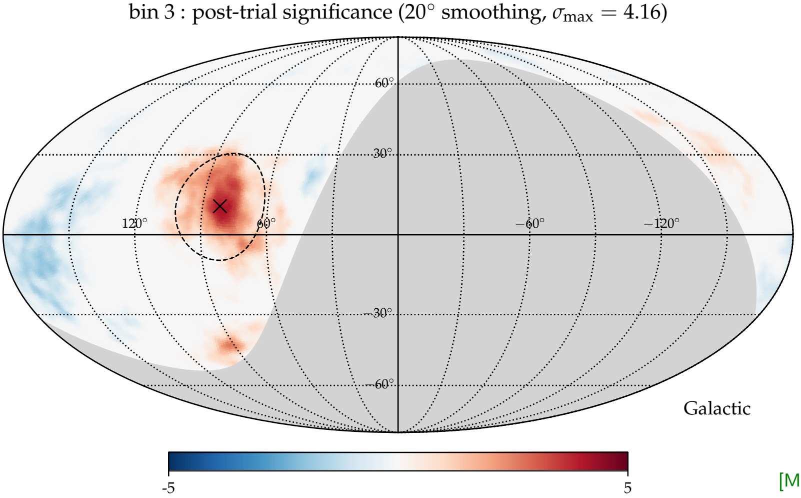

[MA'19]

Small-scale anisotropy of 33 PeV cosmic rays overlaps with Cygnus region.
(gyro radius < 10 pc; neutron decay length $\simeq 300$ pc)

Work in Progress: Rigidity-Dependent KG Analysis

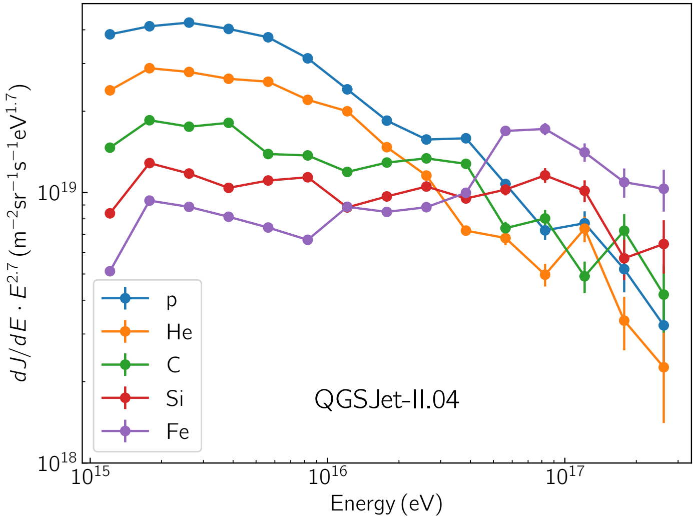

[Kostuin, Plokhikh, MA, *et al.* PoS(ICRC2021)319]

Work in Progress: Rigidity-Dependent KG Analysis

QGSJET-II-04 / $10^{15.5}\mathrm{V} \leq \mathcal{R} \leq 10^{16.0}\mathrm{V}$: anisotropy (45° smoothing)

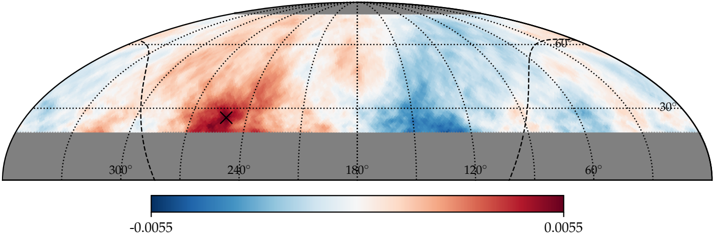

QGSJET-II-04 / $10^{15.5}\mathrm{V} \leq \mathcal{R} \leq 10^{16.0}\mathrm{V}$: pre-trial significance (45° smoothing, $\sigma_{\max} = 2.60$)

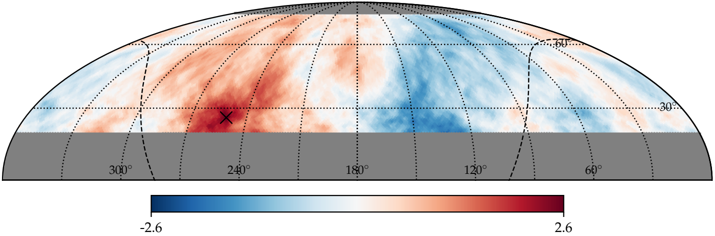

[Kostuin, Plokhikh, MA, *et al.* PoS(ICRC2021)319]

Summary

- Observation of CR anisotropies at the level of **one-per-mille** is challenging.
- Reconstruction methods can **introduce bias**, sometimes not stated or corrected for.
- **Dipole anisotropy** can be understood in the context of standard diffusion theory:
  - TeV-PeV dipole phase aligns with local ordered magnetic field
  - ✔ **New method of measuring local magnetic fields**
  - Amplitude variations as a result of local sources
  - Plausible & natural candidate: **the Vela supernova remnant**
  - ? What is the expected dipole anisotropy in the PV–EV rigidity range?
- Observed CR data shows evidence of **small-scale anisotropy**.
  - ✘ Induces cross-talk with dipole anisotropy in limited field of view
  - ✔ **Probe of local Galactic environment**
  - ? What can learn about our heliosphere from TV small-scale features?
  - ? What is the effect of local ($\lesssim 10$ pc) magnetic turbulence?
  - ? How do we disentangle global CR transport features from local turbulence?

Appendix

Evolution Model

- Diffusion theory motivates that each $\langle C_\ell \rangle$ decays exponentially with an effective **relaxation rate** [Yosida'49]

$$\nu_\ell \propto \mathbf{L}^2 \propto \ell(\ell+1)$$

- A **linear** $\langle C_\ell \rangle$ evolution equation with generation rates $\nu_{\ell\to\ell'}$ requires:

$$\partial_t \langle C_\ell \rangle = -\nu_\ell \langle C_\ell \rangle + \sum_{\ell' \geq 0} \nu_{\ell' \to \ell} \frac{2\ell'+1}{2\ell+1} \langle C_{\ell'} \rangle \quad \text{with} \quad \nu_\ell = \sum_{\ell' \geq 0} \nu_{\ell \to \ell'}$$

- For $\nu_\ell \simeq \nu_{\ell\to\ell+1}$ and $\widetilde{C}_\ell = 0$ for $l \geq 2$ this has the analytic solution:

$$\langle C_\ell \rangle(T) \simeq \frac{3\widetilde{C}_1}{2\ell+1} \prod_{m=1}^{\ell-1} \nu_m \sum_n \prod_{p=1(\neq n)}^{\ell} \frac{e^{-T\nu_n}}{\nu_p - \nu_n}$$

- For $\nu_\ell \simeq \ell(\ell+1)\nu$ we arrive at a finite asymptotic ratio:

$$\lim_{T\to\infty} \frac{\langle C_\ell \rangle(T)}{\langle C_1 \rangle(T)} \simeq \frac{18}{(2\ell+1)(\ell+2)(\ell+1)}$$

Non-Uniform Pitch-Angle Diffusion

- stationary pitch-angle diffusion ($\mu \equiv \cos\theta$) :

$$v\mu \frac{\partial}{\partial z}\langle f\rangle = \frac{\partial}{\partial \mu} D_{\mu\mu} \frac{\partial}{\partial \mu}\langle f\rangle$$

- **non-uniform** diffusion:

$$\frac{D_{\mu\mu}}{1-\mu^2} \neq \text{const}$$

- non-uniform pitch-angle diffusion modifies the large-scale anisotropy aligned with $\mathbf{B}_0$

  - small scale excess/deficits for enhanced diffusion towards $\mu \simeq \pm 1$

    [Malkov, Diamond, Drury & Sagdeev'10]

  - modified large-scale features for enhanced diffusion at $\mu \simeq 0$ [Giacinti & Kirk'17]

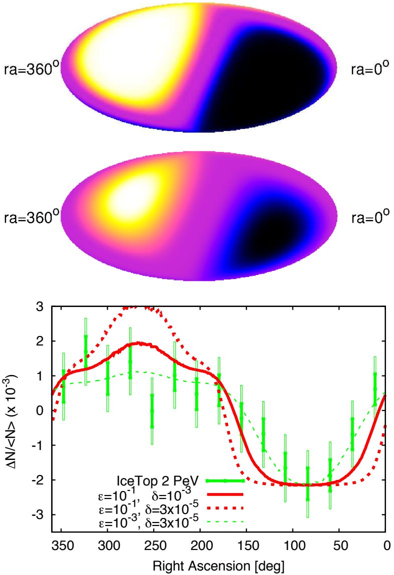

[Giacinti & Kirk'17]

Solar Potential

- dipole anisotropy induced by CR diffusion in solar wind:

$$|\mathbf{\Phi}| = -\underbrace{\frac{\beta_\odot(r)}{3}\frac{\partial\phi}{\partial\ln p}}_{\text{Compton-Getting}} \underbrace{-\kappa_\odot(r,p)\frac{\partial\phi}{\partial r}}_{\text{diffuse dipole}}$$

➜ **force-field approximation**: $|\mathbf{\Phi}| \simeq 0$ [Gleeson & Axford'68;Gleeson & Urch'73]

- local solution related to distribution beyond heliosphere:

$$\phi(r_\oplus, p(r_\oplus)) = \lim_{R\to\infty}\phi(R, p(R))$$

- $p(r)$ solution of **characteristic equation**:

$$\frac{\partial p}{\partial r} = \frac{\beta_\odot(r)}{3}\frac{p}{\kappa_r(r,p)}$$

➜ assume **Bohm diffusion** in heliosphere: $\kappa_\odot(r,p) \simeq \kappa_0(r)(\mathcal{R}/\mathcal{R}_0)$

$$p(r_\oplus) = p(\infty) - |Z|eV_\odot \qquad \text{with} \qquad V_\odot = \underbrace{\frac{\mathcal{R}_0}{3}\int_{r_\oplus}^{\infty} \mathrm{d}r' \frac{\beta_\odot(r')}{\kappa_0(r')}}_{\text{effective ``solar potential''}} \lesssim 1\,\mathrm{GV}$$

Simulated Turbulence

- 3D-isotropic turbulence: [Giacalone & Jokipii'99]

$$\delta\mathbf{B}(\mathbf{x}) = \sum_{n=1}^{N} A(k_n)(\mathbf{a}_n \cos\alpha_n + \mathbf{b}_n \sin\alpha_n)\cos(\mathbf{k}_n\mathbf{x} + \beta_n)$$

- α_n and β_n are random phases in $[0, 2\pi)$, unit vectors $\mathbf{a}_n \propto \mathbf{k}_n \times \mathbf{e}_z$ and $\mathbf{b}_n \propto \mathbf{k}_n \times \mathbf{a}_n$
- with amplitude

$$A^2(k_n) = \frac{2\sigma^2 B_0^2 G(k_n)}{\sum_{n=1}^{N} G(k_n)} \qquad \text{with} \qquad G(k_n) = 4\pi k_n^2 \frac{k_n \Delta\ln k}{1 + (k_n L_c)^\gamma}$$

- Kolmogorov-type turbulence: $\gamma = 11/3$
- $N = 160$ wavevectors $\mathbf{k}_n$ with $|\mathbf{k}_n| = k_{\min} e^{(n-1)\Delta\ln k}$ and $\Delta\ln k = \ln(k_{\max}/k_{\min})/N$
- $\lambda_{\min} = 0.01 L_c$ and $\lambda_{\max} = 100 L_c$ [Fraschetti & Giacalone'12]
- rigidity: $r_L = 0.1 L_c$
- turbulence level: $\sigma^2 = \mathbf{B}_0^2/\langle\delta\mathbf{B}^2\rangle = 1$

Systematic Uncertainty of CR Dipole

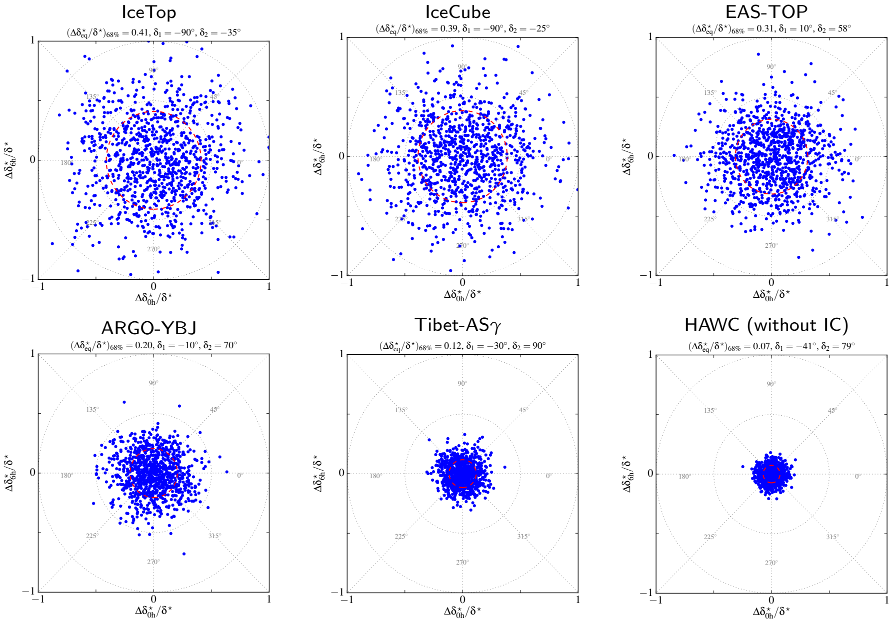

Compton-Getting Effect

- phase-space distribution is **Lorentz-invariant**

$$f(\mathbf{p}) = f^\star(\mathbf{p}^\star)$$

- **relative motion of observer** ($\boldsymbol{\beta} = \mathbf{v}/c$) in plasma rest frame ($\star$):

$$\mathbf{p}^\star = \mathbf{p} + p\boldsymbol{\beta} + \mathcal{O}(\beta^2)$$

- Taylor expansion:

$$f(\mathbf{p}) \simeq f^\star(\mathbf{p}) + (\mathbf{p}^\star - \mathbf{p})\nabla_{\mathbf{p}^\star} f^\star(\mathbf{p}) + \mathcal{O}(\beta^2) \simeq f^\star(\mathbf{p}) + p\boldsymbol{\beta}\nabla_{\mathbf{p}^\star} f^\star(\mathbf{p}) + \mathcal{O}(\beta^2)$$

➜ dipole term $\boldsymbol{\Phi}$ is **not invariant**:

$$\phi = \phi^\star \qquad \text{and} \qquad \boldsymbol{\Phi} = \boldsymbol{\Phi}^\star + \frac{1}{3}\boldsymbol{\beta}\frac{\partial \phi^\star}{\partial \ln p}$$

- with $\phi \sim p^{-2} n_{\rm CR} \propto p^{-2-\Gamma_{\rm CR}}$:

$$\boldsymbol{\delta} = \boldsymbol{\delta}^\star + \underbrace{(2+\Gamma_{\rm CR})\boldsymbol{\beta}}_{\text{Compton-Getting effect}}$$

✘ What is the plasma rest-frame? LSR or ISM : $v \simeq 20\text{km/s}$

Local Sources

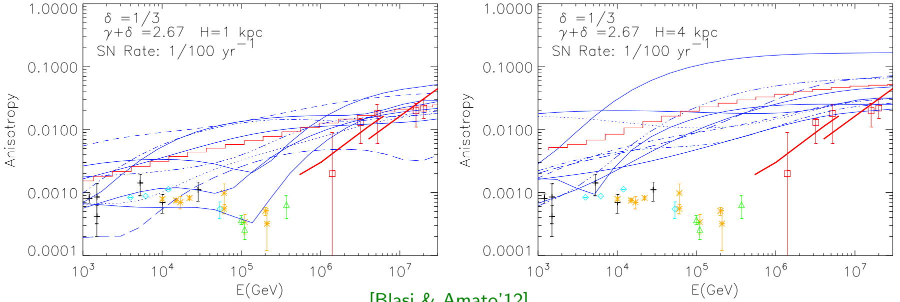

[Blasi & Amato'12]

- Distribution of local cosmic ray sources (SNR) in position and time induces variation in the anisotropy. [Erlykin & Wolfendale'06; Blasi & Amato'12] [Sveshnikova *et al.*'13; Pohl & Eichler'13]
- variance of amplitude can be estimated as: [Blasi & Amato'12]

$$\sigma_A \propto \frac{K(E)}{cH} \qquad \rightarrow \qquad \frac{\sigma_A}{A} = \text{const}$$

Local Magnetic Field

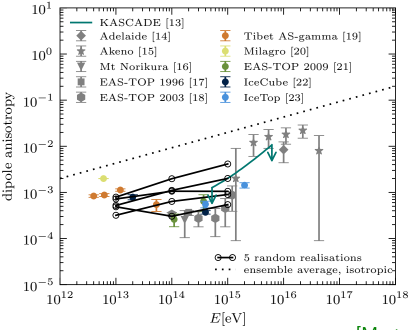

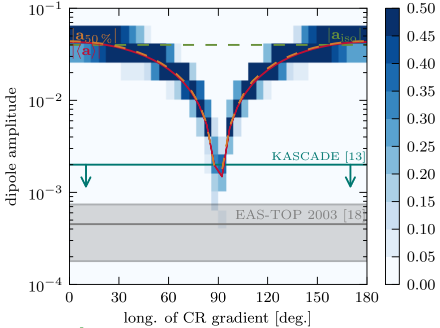

[Mertsch & Funk'14]

- **strong regular magnetic fields** in the local environment

➜ diffusion tensor reduces to **projector**: [*e.g.* Mertsch & Funk'14; Schwadron *et al.*'14; MA'17]

$$K_{ij} \to \kappa_{\parallel} \widehat{B}_i \widehat{B}_j$$

➜ **reduced** dipole amplitude and alignment with magnetic field: $\delta \parallel \mathbf{B}$

Local Magnetic Field

- **IBEX ribbon**: enhanced emission of energetic neutral atoms (ENAs) observed with Interstellar Boundary EXplorer [McComas *et al.*'09]
- interpreted as local magnetic field ($\lesssim 0.1$ pc) drapping the heliosphere
- circle center defines field orientation (in Galactic coordinate system): [Funsten *et al.*'13]

$$l \simeq 210.5^\circ \quad \& \quad b \simeq -57.1^\circ$$
$$(\Delta\theta \simeq 1.5^\circ)$$

- consistent with starlight polarization by interstellar dust ($\lesssim 40$ pc) [Frisch *et al.*'15]

$$l \simeq 216.2^\circ \quad \& \quad b \simeq -49.0^\circ$$

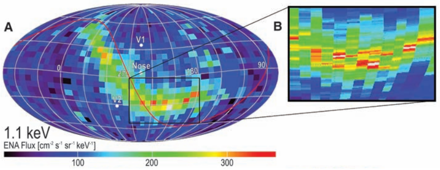

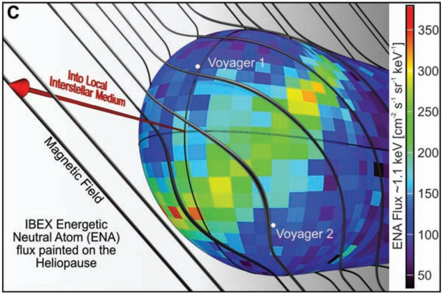

[McComas *et al.*'09]